Theory of giant Raman scattering from semicontinuous metal films

F. Brouers and S. Blacher
Etude Physique des Matériaux et Genie Chimique Université de Liége B5, 4000 Liege, Belgium

A. N. Lagarkov and Andrey K. Sarychev
Center for Applied Problems of Electrodynamics, Russian Academy of Sciences, Izhorskaya St. 13/19, Moscow 127412, Russia

Patrice Gadenne
Laboratorie de Magnetisme et d'Optique de Versailles, Universite de Versailles Saint-Quentin, 45 avenue des Etats Unis, 78035 Versailles Cedex, France

Vladimir M. Shalaev
Department of Physics, New Mexico State University, Las Cruces, New Mexico 88003
(Received 12 November 1996)

The local electric fields in a semicontinuous metal film are shown to exhibit giant fluctuations in the visible and infrared spectral ranges, when the dissipation in metallic grains is small. The field fluctuations result in significantly enhanced Raman scattering from semicontinuous metal films. The scaling analysis is performed to describe giant Raman scattering in the vicinity of the percolation threshold. A theory of Raman scattering from these films is developed. A numerical method based on the theory is suggested and used to calculate Raman scattering from silver semicontinuous films. Results of the simulations are compared with recent experimental observations. [S0163-1829(97)03119-6]

I. INTRODUCTION

The optical properties of metal-insulator thin films have been intensively studied both experimentally and theoretically. Semicontinuous metal films with a two-dimensional (2D) morphology are usually produced by thermal evaporation or sputtering of metal onto an insulating substrate. In the growing process, first, small metallic grains are formed on the substrate. As the film grows, the metal filling factor increases and coalescences occur, so that irregularly shaped clusters are formed on the substrate, resulting in 2D fractal structures. The sizes of these structures diverge in the vicinity of the percolation threshold. A percolating cluster of metal is eventually formed, when a continuous conducting path appears between the ends of the sample. The metal-insulator transition (the percolation threshold) is very close to this point, even in the presence of quantum tunneling. At higher surface coverage, the film is mostly metallic, with voids of irregular shapes. As further coverage increases, the film becomes uniform.

The optical properties of metal-dielectric films show anomalous phenomena that are absent for bulk metal and dielectric components. For example, the anomalous absorption in the near-infrared spectral range leads to unusual behavior of the transmittance and reflectance. Typically, the transmittance is much higher than that of continuous metal films, whereas the reflectance is much lower (see Refs. 1–7, and references therein). Near and well below the conductivity threshold, the anomalous absorptance can be as high as 50%.[6,8–10] A number of effective-medium theories were proposed for calculation of the optical properties of semicontinuous random films, including the Maxwell-Garnett[11] and Bruggeman[12] approaches and their various modifications.[5–7,13] The renormalization group method is also widely used to calculate effective dielectric response of 2D percolating films near the percolation threshold (see Refs. 14 and 15, and references therein). However, none of these theories allows one to calculate the field fluctuations and the effects resulting from these fluctuations.

This paper is concerned with the large local electromagnetic (em) fields that arise in surface-enhanced Raman scattering — one of the most intriguing optical effects discovered in the past 20 years (see, for example, Refs. 16 and 17). Strong fluctuations of the local fields play an important role in enhancements of a variety of nonlinear optical effects, such as four-wave mixing, nonlinear absorption and refraction, harmonic generation, etc.[17,18] The field fluctuations tend to increase significantly Rayleigh scattering from inhomogeneous media.[17,19–21] The enhancements of the near-zone fields can trigger the optical bistability that may be considered as optical analog of the electric transistor with all the basic logic elements.[22] Recently, the near-field fluctuations were directly imaged by using scanning near-field optical microscopy.[23,24] Because semicontinuous metal films are of great interest in terms of their fundamental physical properties and various applications, it is important to study statistical properties of the electromagnetic fields in the near zone of these films. In this paper we study the near-field fluctuations and enhanced Raman scattering resulting from these fluctuations.

To simplify theoretical considerations, we assume below that the electric field is homogeneous in the direction perpendicular to the film plane. This assumption means that the skin depth for the metal grains, $\delta \cong c/(\omega\sqrt{|\varepsilon_m|})$, is much larger than the grain size a_0, so that the quasistatic approximation holds. Note that the role of the skin effect can be very im-

 © 1997 The American Physical Society

portant, resulting, in many cases, in strong alterations of the electromagnetic response found in the quasistatic approximation.[25–28] Yet, the quasistatic approximation significantly simplifies theoretical considerations of the field fluctuations and describes well the optical properties of semicontinuous films providing qualitative (and in some cases, quantitative) agreement with experimental data.[5,29–31]

Below, we neglect the skin effect so that a semicontinuous film can be considered as a 2D object. In the optical frequency range, when the frequency ω is much larger than the relaxation rate τ^{-1} of the metallic component, a semicontinuous metal film can be modeled as a 2D L-R—C lattice.[5,29–31] The capacitance C stands for the gaps between metal grains that are filled by dielectric material (substrate), with the dielectric constant ε_d. The inductive elements, L-R, represent the metallic grains that for the Drude metal have the dielectric function

$$\varepsilon_m(\omega)=\varepsilon_b-(\omega_p/\omega)^2/(1+i\omega_\tau/\omega), \tag{1}$$

where ε_b is a contribution to ε due to interband transitions, ω_p is the plasma frequency, and $\omega_\tau=1/\tau\ll\omega_p$ is the relaxation rate. In the high-frequency range considered here, the losses in metal grains are small, $\omega\gg\omega_\tau$. Therefore the real part of the metal dielectric function is much larger (in modulus) than the imaginary part and it is negative for the frequencies ω below the renormalized plasma frequency, $\omega_p^*=\omega_p/\sqrt{\varepsilon_b}$. Thus the metal conductivity is almost purely imaginary and metal grains can be modeled as the L-R elements, with the active component much smaller than the reactive one.

If the skin effect cannot be neglected, i.e., the skin depth δ is smaller than the metal grain size a_0, the simple quasistatic presentation of a semicontinuous film as a 2D array of the L-R and C elements is not valid. Still, we can use the L-R — C model in the other limiting case, when the skin effect is very strong, $\delta\ll a_0$.[25,26] In this case, the losses in metal grains are small, regardless of the ratio ω/ω_τ, whereas the effective inductance for a metal grain depends on the grain size and shape rather than on the material constants for the metal. In this paper we restrict our consideration to the quasistatic case.

The effective properties of the 2D L-R — C lattices have been intensively studied during the last decade.[5,29–31] However, there was not much attention paid to the fact that the spatial distributions of the local fields in such systems can exhibit rich nontrivial behavior.

It is instructive to consider first the film properties at the percolation threshold p_c, where the exact result for the effective dielectric constant ε_e holds in the quasistatic case:[32] $\varepsilon_e=\sqrt{\varepsilon_d\varepsilon_m}$. If we neglect the metal losses and set $\omega_\tau=0$, the metal-dielectric constant ε_m is negative for frequencies smaller than the renormalized plasma frequency ω_p^*. We also neglect possible small losses in a dielectric substrate, assuming that ε_d is real and positive. Then, ε_e is purely imaginary for $\omega<\omega_p^*$. Therefore a film consisting of loss-free metal and dielectric grains is absorptive for $\omega<\omega_p^*$. The effective absorption in a loss-free film means that the electromagnetic energy is stored in the system and thus the local fields could increase unlimitedly. In reality, the local fields in a metal film are, of course, finite because of the losses. If the losses are small, one anticipates very strong field fluctuations. In this paper we develop a theory of Raman scattering enhanced by the strong fluctuations of the local fields.

Surface-enhanced Raman scattering (SERS) from rough thin films is commonly associated with excitation of surface plasmon oscillations (see, e.g., Refs. 16 and 33). Plasmon oscillations are typically considered in the two limiting cases: (1) oscillations in independent (noninteracting) roughness features of various shapes and (2) surface plasmon waves (polaritons) that laterally propagate along the metal surface (see Refs. 16 and 33, and references therein). In reality, there are strong light-induced interactions between different features of a rough surface and therefore plasmon oscillations should be treated as collective surface excitations (eigenmodes) that depend strongly on the surface morphology. Recently, such an approach was applied by Shalaev *et al.* for description of the optical properties of random self-affine thin films[34] and Raman scattering from such films.[35] Self-affine thin films are produced, for example, by depositing an atomic beam onto a *cold* substrate.[36,37] Contrary to the case of ''usual'' roughness, there is no correlation length for self-affine surfaces. This means that the inhomogeneities of all sizes are present in a self-affine film according to a power-law distribution.[38] The eigenmodes of a self-affine surface are extremely inhomogeneous and tend to be localized.[34] The localized areas with high local fields lead to giant field fluctuations and they are primarily responsible for the enhanced Raman scattering from rough self-affine thin films.[18,35] A qualitatively similar picture of SERS in random small-particle composites (including fractal ones) in a 3D space was earlier suggested in Ref. 18.

The self-affine surfaces described above (as well as small-particle composites) should be considered as 3D objects. Brouers, Blacher, and Sarychev obtained similar results for the field distributions on a 2D semicontinuous metal film.[20,21] As in the case of disordered 3D systems, on a 2D semicontinuous film, giant fluctuations of the electromagnetic fields were predicted in Refs. 20 and 21. It was shown that the fluctuations are very inhomogeneous and highly correlated in space. A correlation length ξ_e was introduced in Refs. 20 and 21; by definition, ξ_e is the length scale within which electric fields at different points of a film are correlated. In Refs. 20 and 21 it was also shown that the smaller the losses in metal grains, the larger the correlation length ξ_e; furthermore, a critical exponent ν_e was introduced for characterization of the divergence of ξ_e, occurring when a metal component of the film is loss-free. (Note that the correlation length ξ_e describes the *field* fluctuations and has nothing to do with the percolation correlation length ξ_p that has a purely geometric meaning.)

In this paper we investigate the field fluctuations in semicontinuous metal films and the enhancement of Raman scattering associated with these fluctuations. First, we present a theory that expresses the enhancement of Raman scattering in terms of the local field fluctuations. It turns out that the enhancement A is simply proportional to the fourth power of the local fields multiplied by the local conductivity squared and averaged over a random film. We develop a very efficient method for calculating the local fields; the method is based on the real space renormalization group approach. We use this method to find the field fluctuations and Raman scat-

tering from silver semicontinuous films and show that for $\omega < \omega_p^*$ (for silver, ω_p^* corresponds to $\lambda_p^* \approx 0.3$ μm) Raman scattering can be enhanced, on average, by more than five orders of magnitude, in the vicinity of the percolation threshold. The enhancement remains large in the far-infrared range up to $\lambda \leqslant 100$ μm. This enhancement is explained by using the percolation theory. We determine the scaling behavior of Raman scattering and provide simple analytical estimations for the enhancement and the concentration range near the percolation threshold where the enhancement occurs. We also compare our calculations with recent experimental observations.[39] In the end, we summarize the obtained results.

II. THEORY OF RAMAN SCATTERING FROM INHOMOGENEOUS MEDIA

We consider the optical properties of a semicontinuous film consisting of metal grains randomly distributed on a dielectric substrate. The film is placed in the $\{x,y\}$ plane, whereas the incident wave propagates in the z direction. The local conductivity $\sigma(\mathbf{r})$ of the film takes either the ''metallic'' values, $\sigma(\mathbf{r})=\sigma_m$, in the metal grains or the ''dielectric'' values, $\sigma(\mathbf{r})=-i\omega\varepsilon_d/4\pi$, outside the metal grains. The vector $\mathbf{r}=\{x,y\}$ has two components in the plane of the film; ω is the frequency of the incident wave. The gaps between metallic grains are filled by the material of the substrate, so that the ε_d introduced above is equal to the dielectric constant of the substrate. We assume that the electric field in the film is homogeneous in the direction z perpendicular to the film plane; this means that the skin depth for the metal, $\delta \cong c/(\omega\sqrt{|\varepsilon_m|})$, is much larger than the metal grain size a_0, and the quasistatic approximation can be applied for calculating the field distributions. We also take into account that the wavelength of the incident wave is much larger than any characteristic size of the film, including the grain size, the gaps between the grains, etc. In this case, the local field $\mathbf{E}(\mathbf{r})$ can be represented as

$$\mathbf{E}(\mathbf{r}) = -\nabla\phi(\mathbf{r}) + \mathbf{E}_e(\mathbf{r}), \tag{2}$$

where $\mathbf{E}_e(\mathbf{r})$ is the external applied field [to be exact, $\mathbf{E}_e(\mathbf{r})$ is the macroscopic field; see discussion at the end of this section], and $\phi(\mathbf{r})$ are the local potentials of the fluctuating fields inside the film. The current density $\mathbf{j}(\mathbf{r})$ at point $\mathbf{r}$ is given by Ohm's law,

$$\mathbf{j}(\mathbf{r}) = \sigma(\mathbf{r})[-\nabla\phi(\mathbf{r}) + \mathbf{E}_e(\mathbf{r})]. \tag{3}$$

The current conservation law, $\nabla\cdot\mathbf{j}(\mathbf{r})=0$, has the form

$$\nabla\cdot\{\sigma(\mathbf{r})[-\nabla\phi(\mathbf{r}) + \mathbf{E}_e(\mathbf{r})]\} = 0. \tag{4}$$

We solve Eq. (4) to find the fluctuating potentials $\phi(\mathbf{r})$ and the local fields $\mathbf{E}(\mathbf{r})$ induced in the film by the external field $\mathbf{E}_e(\mathbf{r})$.

It is instructive to assume first that the external field $\mathbf{E}_e(\mathbf{r})$ is pinlike, $\mathbf{E}_e(\mathbf{r}) = \mathbf{E}_1\delta(\mathbf{r}-\mathbf{r}_1)$, where the $\delta(\mathbf{r})$ is the Dirac delta function. The current density at arbitrary point $\mathbf{r}_2$ is given by the linear relation

$$\mathbf{j}(\mathbf{r}_2) = \hat{S}(\mathbf{r}_2,\mathbf{r}_1)\mathbf{E}_1, \tag{5}$$

defining the nonlocal conductivity matrix $\hat{S}(\mathbf{r}_2,\mathbf{r}_1)$. This matrix represents the system response at point $\mathbf{r}_2$ to the field source located at point $\mathbf{r}_1$. The nonlocal conductivity $\hat{S}$ can be expressed in terms of the Green function G of Eq. (4):

$$\nabla\cdot\{\sigma(\mathbf{r}_2)[\nabla G(\mathbf{r}_2,\mathbf{r}_1)]\} = \delta(\mathbf{r}_2-\mathbf{r}_1), \tag{6}$$

where the differentiation with respect to the coordinate $\mathbf{r}_2$ is assumed.

Comparing Eqs. (4) and (6) and using the definition of the nonlocal conductivity given in Eq. (5), we obtain (see the Appendix)

$$S^{\alpha\beta}(\mathbf{r}_2,\mathbf{r}_1) = \sigma(\mathbf{r}_2)\sigma(\mathbf{r}_1)\frac{\partial^2 G(\mathbf{r}_2,\mathbf{r}_1)}{\partial r_2^\alpha \partial r_1^\beta}, \tag{7}$$

where the Greek indices take values 1 or 2. As follows from the symmetry of Eq. (6), the Green function is symmetric with respect to the interchange of its arguments: $G(\mathbf{r}_1,\mathbf{r}_2) = G(\mathbf{r}_2,\mathbf{r}_1)$. Then, Eq. (7) implies that the nonlocal conductivity is also symmetric:

$$S^{\alpha\beta}(\mathbf{r}_1,\mathbf{r}_2) = S^{\beta\alpha}(\mathbf{r}_2,\mathbf{r}_1). \tag{8}$$

The introduction of the nonlocal conductivity $\hat{S}$ considerably simplifies further calculations of the local field distributions. The symmetry of $\hat{S}$ given by Eq. (8) is also important for the following analysis.

Since the wavelength of the incident em wave is much larger than all spatial scales in a semicontinuous metal film, the external field $\mathbf{E}_e$ is constant in the film plane, $\mathbf{E}_e(\mathbf{r}) = \mathbf{E}_0$. The local fields $\mathbf{E}(\mathbf{r}_2)$ induced by the external field $\mathbf{E}_0$ can be obtained by using the definition (5) for the nonlocal conductivity $\hat{S}$ as follows:

$$\mathbf{E}(\mathbf{r}_2) = \frac{1}{\sigma(\mathbf{r}_2)}\int \hat{S}(\mathbf{r}_2,\mathbf{r}_1)\mathbf{E}_0 d\mathbf{r}_1. \tag{9}$$

The local fields $\mathbf{E}(\mathbf{r}_2)$ excite Raman-active molecules that are assumed to be uniformly distributed over the film. The Raman-active molecules, in turn, generate the Stokes fields, $\mathbf{E}_s(\mathbf{r}_2) = \kappa(\mathbf{r}_2)\mathbf{E}(\mathbf{r}_2)$, oscillating at the shifted frequency ω_s [$\kappa(\mathbf{r}_2)$ is the ratio for the Raman and linear polarizabilities of the Raman-active molecule at the point $\mathbf{r}_2$]. The Stokes fields $\mathbf{E}_s(\mathbf{r}_2)$ induce in the film currents $\mathbf{j}_s(\mathbf{r}_3)$ that are given by the equation similar to Eq. (9):

$$\mathbf{j}_s(\mathbf{r}_3) = \int \hat{S}(\mathbf{r}_3,\mathbf{r}_2)\mathbf{E}_s(\mathbf{r}_2) d\mathbf{r}_2. \tag{10}$$

Since the Stokes-shifted frequency ω_s is typically very close to the frequency of the external field, $|\omega-\omega_s|/\omega \ll 1$, we can set the nonlocal conductivities $\hat{S}$ appearing in Eqs. (9) and (10) to be the same.

The intensity of the electromagnetic wave, I, scattered from any inhomogeneous system is proportional to the current fluctuations inside the system,

$$I \propto \left\langle \left| \int [\mathbf{j}(\mathbf{r}) - \langle \mathbf{j}\rangle] d\mathbf{r} \right|^2 \right\rangle, \tag{11}$$

where the integration is over the entire system and the angular brackets, $\langle\ \rangle$, denote the ensemble average. For Raman

scattering, the mean includes averaging over the fluctuating phases of the incoherent Stokes fields generated by different Raman-active molecules. Therefore the averaged current density oscillating at ω_s is zero, $\langle \mathbf{j}_s \rangle = 0$. Then, the intensity of Raman scattering, I_s, from a semicontinuous metal film acquires the form

$$I_s \propto \left\langle \left| \int \mathbf{j}(\mathbf{r}) d\mathbf{r} \right|^2 \right\rangle = \int \langle S^{\alpha\beta}(\mathbf{r}_3,\mathbf{r}_2)\kappa(\mathbf{r}_2)\mathbf{E}^{\beta}(\mathbf{r}_2) \times S^{*\alpha\gamma}(\mathbf{r}_5,\mathbf{r}_4)\kappa^*(\mathbf{r}_4)\mathbf{E}^{*\gamma}(\mathbf{r}_4)\rangle \times d\mathbf{r}_2 d\mathbf{r}_3 d\mathbf{r}_4 d\mathbf{r}_5, \tag{12}$$

where the summation over repeating Greek indices is implied. All the integrations in Eq. (12) are over the entire film plane.

Since the Raman field sources are incoherent, we have

$$\langle \kappa(\mathbf{r}_2)\kappa^*(\mathbf{r}_4)\rangle = |\kappa|^2 \delta(\mathbf{r}_2 - \mathbf{r}_4), \tag{13}$$

and Eq. (12) takes the form

$$I_s \propto \int \langle S^{\alpha\beta}(\mathbf{r}_3,\mathbf{r}_2) S^{*\mu\gamma}(\mathbf{r}_5,\mathbf{r}_2)\delta^{\alpha\mu}|\kappa|^2 \mathbf{E}^{\beta}(\mathbf{r}_2)\mathbf{E}^{*\gamma}(\mathbf{r}_2)\rangle \times d\mathbf{r}_2 d\mathbf{r}_3 d\mathbf{r}_5, \tag{14}$$

where we introduced the Kronecker symbol $\delta^{\alpha\mu}$ to simplify further considerations. Since a semicontinuous film is macroscopically homogeneous, Raman scattering is independent of the orientation of the external field $\mathbf{E}_0$; therefore we can average Eq. (12) over the orientations of the $\mathbf{E}_0$ without changing the result. The averaging of the products $E^{\beta}(\mathbf{r}_2)E^{*\gamma}(\mathbf{r}_2)$ and $E_0^{\beta}E_0^{*\gamma}$ results in the expressions

$$\langle E^{\beta}(\mathbf{r}_2)E^{*\gamma}(\mathbf{r}_2)\rangle_0 = \frac{1}{2}\langle |E(\mathbf{r}_2)|^2\rangle_0 \delta^{\beta\gamma}, \tag{15}$$

$$\delta^{\alpha\mu} = 2\frac{\langle E_0^{\alpha}E_0^{*\mu}\rangle_0}{|E_0|^2}, \tag{16}$$

where $\langle\ \rangle_0$ denotes the orientation averaging. Substituting Eqs. (15) and (16) in Eq. (14) and noting that the nonlocal conductivity $\hat{S}$ is independent of the field orientations, we obtain for the intensity of the Raman signal the result

$$\langle I_s \rangle \propto \int S^{\alpha\beta}(\mathbf{r}_3,\mathbf{r}_2) S^{*\mu\beta}(\mathbf{r}_5,\mathbf{r}_2) \times \frac{\langle E_0^{\alpha}E_0^{*\mu}\rangle_0}{|E_0|^2}|\kappa|^2 \langle |E(\mathbf{r}_2)|^2\rangle_0 d\mathbf{r}_2 d\mathbf{r}_3 d\mathbf{r}_5. \tag{17}$$

(For simplicity, we omit here the sign for the ensemble averaging.) Now we can use the symmetry of the nonlocal conductivity given by Eq. (8) to rewrite Eq. (17) as

$$\langle I_s \rangle \propto \int \langle S^{\beta\alpha}(\mathbf{r}_2,\mathbf{r}_3)E_0^{\alpha} S^{*\beta\mu}(\mathbf{r}_2,\mathbf{r}_5)E_0^{*\mu}\rangle_0 \frac{|\kappa|^2}{|E_0|^2} \times \langle |E(\mathbf{r}_2)|^2\rangle_0 d\mathbf{r}_2 d\mathbf{r}_3 d\mathbf{r}_5. \tag{18}$$

Integrating over the coordinates $\mathbf{r}_3$ and $\mathbf{r}_5$ and using Eq. (9), we obtain

$$\langle I_s \rangle \propto \frac{|\kappa|^2}{|E_0|^2}\int |\sigma(\mathbf{r}_2)|^2 \langle |E(\mathbf{r}_2)|^2\rangle_0 \langle |E(\mathbf{r}_2)|^2\rangle_0 d\mathbf{r}_2. \tag{19}$$

It is easy to show (see the Appendix) that this equation can be rewritten for a macroscopically isotropic system in the form

$$\langle I_s \rangle \propto \frac{|\kappa|^2}{|E_0|^2}\int |\sigma(\mathbf{r}_2)|^2 |E(\mathbf{r}_2)|^4 d\mathbf{r}_2. \tag{20}$$

If there were no metal grains on the film, the local fields would not fluctuate and one would obtain the following expression for Raman scattering:

$$I_s^0 \propto \int |\sigma_d|^2 |\kappa|^2 |E_0|^2 d\mathbf{r}_2. \tag{21}$$

Therefore the enhancement of Raman scattering, A, due to the presence of metal grains on a dielectric substrate, is given by

$$A = \frac{\langle I_s \rangle}{I_s^0} = \frac{\langle |\sigma(\mathbf{r})|^2 |E(\mathbf{r})|^4\rangle}{|\sigma_d|^2 |E_0|^4} = \frac{\langle |\varepsilon(\mathbf{r})|^2 |E(\mathbf{r})|^4\rangle}{\varepsilon_d^2 |E_0|^4}. \tag{22}$$

This result was previously obtained by Shalaev and coworkers for small-particle composites (including fractal ones) embedded in a 3D space[17,18] and for self-affine thin films;[35] the considerations in all these cases were based on the discrete dipole approximation. Here, formula (22) was obtained using a different approach, and it generalizes the previous considerations[17,18,35] for the case of 2D semicontinuous films. Note that the derivation of Eq. (22) is essentially independent of the dimensionality and morphology of a system. Therefore the enhancement of Raman scattering given by Eq. (22) holds for any inhomogeneous system provided the field fluctuations take place inside it. In particular, Eq. (22) gives the enhancement for Raman scattering from a rough metallic surface, provided the wavelength is much larger than the roughness spatial scales; it can also be used to calculate enhancements for Raman scattering in three-dimensional percolation composites. Our theory implies that the main sources for the Raman signal are the currents exited by Raman molecules in the metal grains. This explains why a significant enhancement for Raman scattering is observed even for sufficiently flat metal surfaces.[16,33,40]

We stress that the electric field E_0 that appears in our formalism is the average (macroscopic) field *inside* the film. When the reflectance of the film is not negligible the field E_0 differs from the incident field $E_{\rm inc}$ even in the quasistatic limit. For 2D films, the internal field E_0 can be easily found in terms of the incident field $E_{\rm inc}$. Let a film be placed in the plane $z=0$, and the em wave, with the electric field parallel to the film plane (s polarization), be incident from the $z>0$ semispace at some angle θ to the z axis. The amplitude of the em field in the $z>0$ semispace is equal to

$$\mathbf{E}_>(\mathbf{r},z) = \mathbf{E}_{\rm inc}\exp(-ik_z z - i\mathbf{q}\cdot\mathbf{r}) + R_s(\theta)\mathbf{E}_{\rm inc} \times \exp(ik_z z - i\mathbf{q}\cdot\mathbf{r}), \tag{23}$$

where $\mathbf{E}_{\rm inc}$ is the amplitude of the incident wave, $\mathbf{k}=\{\mathbf{q},k_z\}$, $k_z = k\cos\theta$ is the wave vector of the incident wave, $R_s(\theta)$ is the reflectance of the film for the s polariza-

tion, and $\mathbf{r}=\{x,y\}$ is a vector in the film plane. The field below the film ($z<0$) takes the form

$$\mathbf{E}_{<}(\mathbf{r},z)=T_s(\theta)\mathbf{E}_{\rm inc}\exp(-ik_z z-i\mathbf{q}\cdot\mathbf{r}), \tag{24}$$

where $T_s(\theta)$ is the film transmittance for the s polarization. According to Eq. (24), the field at the back surface of the film can be written as

$$\mathbf{E}_0(\mathbf{r},0)=T_s(\theta)\mathbf{E}_{\rm inc}\exp(-i\mathbf{q}\cdot\mathbf{r}). \tag{25}$$

The same equations are valid for the p-polarized wave. Since we assume that the film thickness is much smaller than the skin depth δ and therefore the field inside the film is homogeneous in the z direction, Eq. (25) actually gives the average electric field inside the film. All relevant scales in the film are supposed to be much smaller than the wavelength, $\lambda\sim 1/q$, and we can omit the factor $e^{-i\mathbf{q}\cdot\mathbf{r}}$, when considering the field distribution in the film. Thus we obtain that the field E_0 is related to the field of the incident wave, $E_{\rm inc}$, as

$$E_0=T_s(\theta)E_{\rm inc} \tag{26}$$

for the s-polarized wave, and

$$E_0=T_p(\theta)E_{\rm inc}\cos\theta \tag{27}$$

for the p polarization. Therefore the enhancement (22) for Raman scattering should be rewritten, in a general case, as

$$A(\theta)_{s,p}=|T(\theta)_{s,p}|^2\frac{\langle|\varepsilon(\mathbf{r})|^2|E(\mathbf{r})|^4\rangle}{\varepsilon_d^2|E_0|^4}. \tag{28}$$

For a purely dielectric film (assumed to be transparent), we obtain from Eq. (28) the expected result, $A=1$.

For the normal incidence, we have

$$E_0=TE_{\rm inc}, \tag{29}$$

where the normal transmittance $T=T_s(0)=T_p(0)$ is given by the well-known equation (see, e.g., Refs. 10 and 19)

$$T=\frac{1}{1+2\pi\sigma_e d/c}\equiv\frac{1}{1-i\pi\varepsilon_e d/\lambda}. \tag{30}$$

Here d is the film thickness, σ_e and ε_e are, respectively, the effective conductivity and the dielectric constant of the film, and λ is the wavelength of the incident wave. Thus for the normal incidence Eq. (28) transforms to

$$A_n=\left|1-i\frac{\pi\varepsilon_e d}{\lambda}\right|^{-2}\frac{\langle|\varepsilon(\mathbf{r})|^2|E(\mathbf{r})|^4\rangle}{\varepsilon_d^2|E_0|^4}. \tag{31}$$

The transmittance of a semicontinuous film is of the order of unity, for sufficiently small metal concentrations $p\ll 1$. It takes the value $T\cong 1/4$ for the concentrations close to the percolation threshold, where the anomalous adsorption is observed.[6,8–10] Therefore the presence of the transmittance factor in Eqs. (28) and (31) does not change much the enhancement of Raman scattering. One can still use Eq. (22) for a qualitative estimation of the enhancement in this concentration range. However, the transmittance vanishes very fast for $p>0.8$, and the Raman signal is also anticipated to decrease, in this case. For a pure metallic film, $p=1$, the transmittance is small $|T_n|^2\approx(\lambda/\pi|\varepsilon_m|d)^2\ll 1$ (Refs. 6 and 8–10) even for the case when the skin effect is negligible considered here. Substituting this result in Eq. (31), we obtain

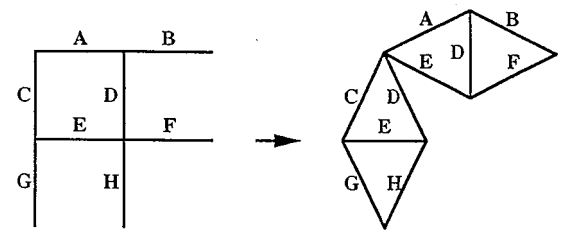

FIG. 1. The real space renormalization scheme.

$$A_n(p=1)=\left(\frac{\lambda}{\pi\varepsilon_d d}\right)^2. \tag{32}$$

Since the wavelength λ is much larger than the film thickness d there is a significant enhancement, even for pure metallic films.

III. NUMERICAL SIMULATIONS FOR FIELD DISTRIBUTIONS IN SEMICONTINUOUS METAL FILMS

To calculate Raman scattering from a semicontinuous metal film, one needs to know the field and current distributions in the film. There exist now very efficient numerical methods for calculating the effective conductivity of composite materials (see Refs. 3 and 5), but they typically do not allow calculations of the field distributions. Here we used instead the real space renormalization group (RSRG) method that was suggested by Reynolds, Klein, and Stanley[41] and Sarychev[42] and then extended to study the conductivity[43] and permeability of oil reservoirs.[44] Below we follow the approach used by Aharony.[44] This method can be adapted to finding the field distributions in the following way. First, we generate a square lattice of the L-R (metal) and C (dielectric) bonds, using a random number generator. As seen in Fig. 1(a), such a lattice can be considered as a set of the ''corner'' elements. One of such elements is labeled as (ABCDEFGH), in Fig. 1(a). In the first stage of the RSRG procedure, each of these elements is replaced by the two Wheatstone bridges, as shown in Fig. 1(b). After this transformation, the initial square lattice is converted to another square lattice, with the distance between the sites two times larger and with each bond between the two nearest neighboring sites being the Wheatstone bridge. Note that there is a one-to-one correspondence between the x bonds in the initial lattice and the x bonds in the x directed bridges of the transformed lattice, as seen in Fig. 1(b). The same one-to-one correspondence exists also between the y bonds. The transformed lattice is also a square lattice, and we can again apply to it the RSRG transformation. We continue this procedure until the size l of the system is reached. As a result, instead of the initial lattice, we have two large Wheatstone bridges in the x and y directions. Each of them has a hierarchical structure consisting of bridges with the sizes from 2 to l. Because the one-to-one correspondence is preserved at each step of the transformation, the correspondence also exists between the

elementary bonds of the transformed lattice and the bonds of the initial lattice.

After using the RSRG transformation, we apply an external field to the system and solve the Kirchhoff equations to determine the fields and the currents in all the bonds of the transformed lattice. Due to the hierarchical structure of the transformed lattice, these equations can be solved exactly. Then, we use the one-to-one correspondence between the elementary bonds of the transformed lattice and the bonds of the initial square lattice to find the field distributions in the initial lattice as well as its effective conductivity. The number of operations to get the full distributions of the local fields is proportional to l^2 (to be compared with l^7 operations needed in the transform-matrix method[5] and l^3 operations needed in the Frank-Lobb algorithm;[45] none of those methods give the local field distributions). With our method, it takes only a few minutes to calculate the effective conductivity and field distributions in a system 1000×1000 using a computer like the Pentium-200.

The RSRG procedure is certainly not exact since the effective connectivity of the transformed system does not repeat exactly the connectivity of the initial square lattice. To check the accuracy of the RSRG, we solved the 2D percolating problem using this method. Namely, we calculated the effective parameters of a two-component composite with the real metallic conductivity σ_m much larger than the real conductivity σ_d of the dielectric component, $\sigma_m \gg \sigma_d$. We obtained the percolation threshold $p_c=0.5$ and the effective conductivity at the percolation threshold that is very close to $\sigma(p_c)=\sqrt{\sigma_m\sigma_d}$. These results coincide with the exact ones for 2D composites.[32] This is not surprising since the RSRG procedure preserves the self-duality of the initial system. The critical exponents obtained by the RSRG are also close to the known values of the exponents from the percolation theory.[5] Therefore we believe that the local fields we obtain here are close to the actual ones.

IV. GIANT FIELD FLUCTUATIONS AND ENHANCEMENT OF RAMAN SCATTERING IN SEMICONTINUOUS METAL FILMS

We use the method described above to calculate the field distributions in silver semicontinuous films and the enhancement of Raman scattering induced by the field fluctuations. We model a film by a square lattice consisting of metallic bonds, with the conductivity $\sigma_m=-i\varepsilon_m\omega/4\pi$ (L-R bonds) and the concentration p, and dielectric bonds with the conductivity $\sigma_d=-i\varepsilon_d\omega/4\pi$ (C bonds) and concentration $1-p$. The external field E_0 is set to be equal to unity, $E_0=1$, whereas the local fields inside the system are complex quantities. The dielectric constant of the silver grains has the form of Eq. (1), with the interband-transition contribution $\varepsilon_b=5$, the plasma frequency $\omega_p=9.1$ eV, and the relaxation frequency $\omega_\tau=0.021$ eV.[46]

The intensities of the local electric fields, $I_2(\mathbf{r})=|E(\mathbf{r})|^2$ and $I_4(\mathbf{r})=|E(\mathbf{r})|^4$, are obtained by the RSRG method, and the results are shown in Figs. 2 and 3, for the wavelengths of the external em field $\lambda=0.5$ μm and $\lambda=20$ μm. The concentration of metal particles, p, is chosen to be equal to the one at the percolation threshold, $p=p_c=0.5$. As seen in the figure, the intensity fluctuations exceed the intensity of the applied field by more than three orders of magnitude, for I_2, and by more than seven orders of magnitude, for I_4. It is worth emphasizing that these giant fluctuations occur in a macroscopically homogeneous system. This kind of fluctuation was likely observed in recent experiments.[24] Previously, giant fluctuations were reported for fractal clusters.[17,18,23,47] The giant fluctuations can result in large enhancements of a number of optical effects.[17]

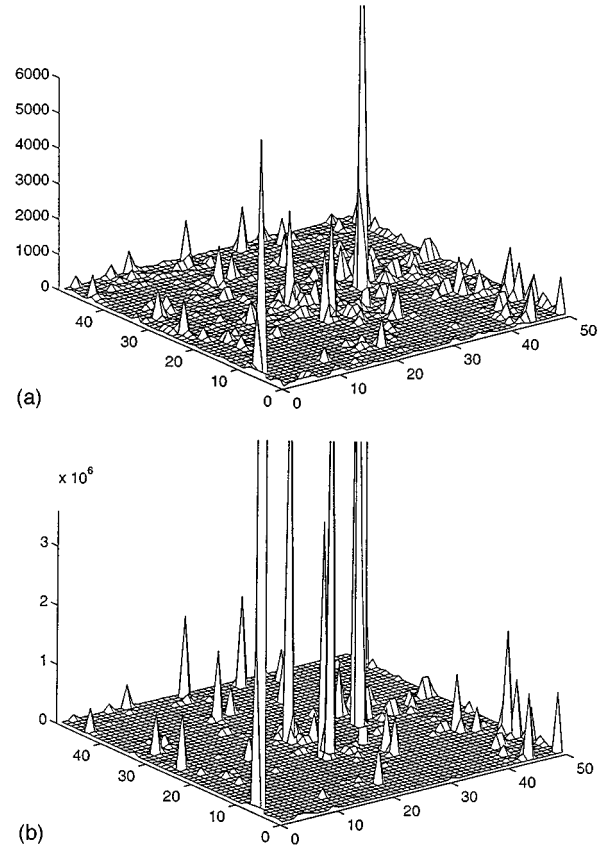

FIG. 2. The electric field intensities on a silver semicontinuous film at the percolation threshold, for the wavelength $\lambda=0.5$ μm; (a) $I_2(\mathbf{r})=|E(\mathbf{r})|^2$ and (b) $I_4(\mathbf{r})=|E(\mathbf{r})|^4$.

Using Eq. (22), we can find the enhancement of Raman scattering for the calculated field distributions. The results are shown in Fig. 4. As seen in the figure, Raman scattering is enhanced by more than five orders of magnitude in the vicinity of the percolation threshold p_c. The enhancement occurs for frequencies smaller than the renormalized plasma frequency, ω_p^*, and it remains very large up to the far infrared.

One could anticipate that the local fields experience giant fluctuations in a semicontinuous film for $\omega\leqslant\omega_p^*$. In this frequency range, the real part of the metal-dielectric constant ε_m is negative and its absolute values are of the order of unity, i.e., they are close to the dielectric constant of the film substrate, ε_d. Therefore the conductivities of the L-R and C elements in the equivalent network have opposite signs and they are close to each other in absolute values. Thus a semicontinuous film, in this case, can be thought of as a system of the contours tuned in resonance with the external field frequency. These resonance modes are seen as giant spatial fluctuations in the field distributions over the film.

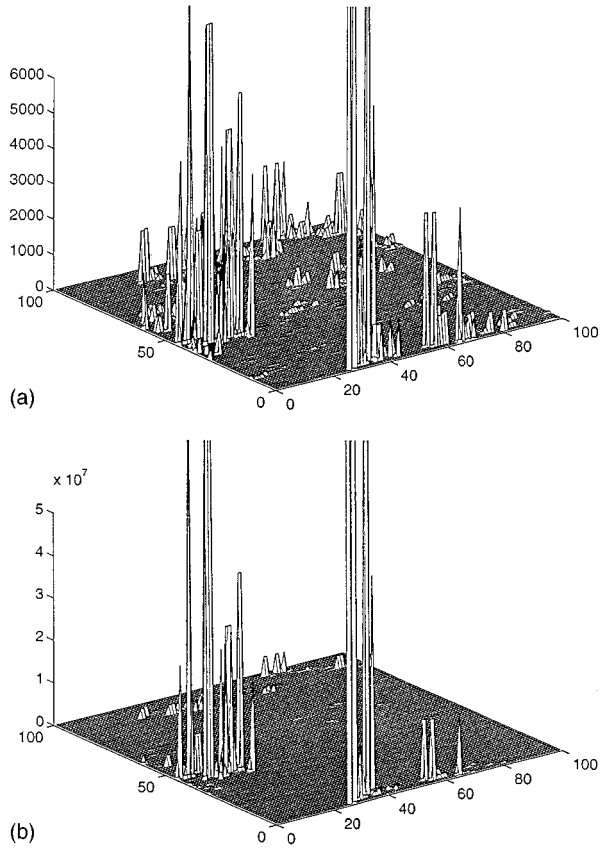

FIG. 3. The electric field intensities on a silver semicontinuous film at the percolation threshold, for the wavelength $\lambda = 20\ \mu$m; (a) $I_2(\mathbf{r}) = |E(\mathbf{r})|^2$ and (b) $I_4(\mathbf{r}) = |E(\mathbf{r})|^4$.

What might be more surprising is the fact that the giant fluctuations of the local fields also occur for $\omega \ll \omega_p^*$, when the contrast $H = |\varepsilon_m|/\varepsilon_d \gg 1$. If the contrast $H \gg 1$, the conductivities of the L-R and C elements of the equivalent network are quite different and a single contour cannot be excited by the external field.

To understand the origin of the giant field fluctuations for the large contrast, $H \gg 1$, we invoke scaling arguments of the

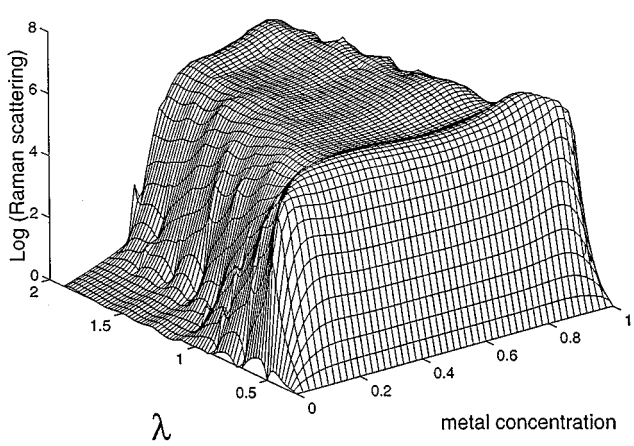

FIG. 4. The enhancement factor A for Raman scattering from a silver semicontinuous film as a function of the metal concentration p and the wavelength λ.

percolation theory.[4] Since Raman scattering has a maximum near the percolation threshold p_c, we assume, for simplicity, that the concentration of the conducting particles, p, is exactly equal to the percolation threshold, $p = p_c$. We consider the case when the frequency ω is much smaller than the plasma frequency, $\omega \ll \omega_p$, so that the contrast can be approximated as $H \approx (\omega_p/\omega)^2/\varepsilon_d \gg 1$. We also assume that $\omega \gg \omega_\tau$, i.e., the losses in the metal grains are relatively small. To find the field distributions over the system, we apply the known renormalization procedure,[41,42] dividing a system in squares of size l and considering each square as a new element. All such squares can be classified by two types. A square that contains a path of conducting particles spanning over is considered a ''conducting'' element. A square without such an ''infinite'' cluster is considered a nonconducting — ''dielectric'' element. Following the finite-size arguments,[3,4] the effective dielectric constant of a ''conducting'' square, $\varepsilon_m^*(l)$, decreases with increasing size l as

$$\varepsilon_m^*(l) = (l/a_0)^{-t/\nu_p} \varepsilon_m, \tag{33}$$

where a_0 is the metal grain size, and t and ν_p are the critical exponents for the conductivity and the percolation correlation length, respectively. For a 2D system, $t \approx \nu_p = 4/3$.[5,30] The effective dielectric constant of the ''dielectric'' square, $\varepsilon_d^*(l)$, increases with increasing size l as

$$\varepsilon_d^*(l) = (l/a_0)^{s/\nu_p} \varepsilon_d, \tag{34}$$

where s is the critical exponent for the static dielectric constant; $s \approx \nu_p = 4/3$ for a 2D system.[5,30]

We now set the square size l to be equal to

$$l = l^* = a_0(|\varepsilon_m'|/\varepsilon_d)^{\nu_p/(t+s)}, \tag{35}$$

where $\varepsilon_m' + i\varepsilon''_m \equiv \mathrm{Re}(\varepsilon_m) + i\,\mathrm{Im}(\varepsilon_m)$. Then, in the renormalized system, where each square of the size l^* is considered as a single element, the ratio of the dielectric constants of these new elements is equal to

$$\varepsilon_m^*(l^*)/\varepsilon_d^*(l^*) \cong \varepsilon_m/|\varepsilon_m'| = -1 + i\kappa, \tag{36}$$

with the loss factor $\kappa = \varepsilon''_m/|\varepsilon_m'| \approx \omega/\omega_\tau \ll 1$. (Recall that in the visible and IR spectral ranges the real part of the metal dielectric constant, ε_m', is negative and large in the absolute values, $|\varepsilon_m'| \gg \varepsilon_d$.)

It follows from Eq. (36) that the renormalized system is a system of the L-R and C elements tuned in the resonance. Therefore the local electric fields $E^*(l^*)$ are significantly enhanced in comparison with the external field E_0. As shown in Refs. 20 and 21, in a 2D system with the ratio of ε_m to ε_d given by Eq. (36), the field E^* can be estimated as

$$E^* \cong E_0 \kappa^{-\gamma/2} \gg E_0, \tag{37}$$

where the critical exponent γ introduced in Refs. 20 and 21 is about unity, $\gamma \cong 1.0$. [Note that for small-particle composites the exact result, with $\gamma = 1$, was proved in Ref. 47; see also, for example, Eq. (7.4) in Ref. 17.]

Now we can estimate the field fluctuations in the original system. The field is still inhomogeneous for scales less than l^*. There are many finite-size metal clusters, even inside a

square of the size l^* that is considered to be a dielectric one. The voltage applied to the square drops mainly in the gaps between the metal clusters. Moreover, the field mainly concentrates at the points where these clusters closely approach each other, so that the distances between the clusters are of the order of the metal grain size a_0. We assume that the number of such points with closest approach of clusters does not depend on the size l since the film is scale invariant at $p=p_c$. A typical voltage drop U^* across a square of the size l^* is approximated as $U^*=E^*l^*$. Therefore the local electric fields $E_{\rm loc}$ concentrated at the points of the closest approach can be estimated as

$$E_{\rm loc}\propto E^*l^*/a_0\simeq E_0(|\varepsilon_m'|/\varepsilon_d)^{\nu_p/(t+s)}\kappa^{-\gamma/2}. \tag{38}$$

Above, we estimated the field fluctuations in the ''dielectric'' squares. The structure of the finite clusters in the ''conducting'' squares is basically the same since the only difference between the two types of squares is the presence of a conducting path through the square. This path does not affect the largest fields inside the squares. In both cases, the fields are mainly concentrated in the gaps between finite clusters. Therefore the field fluctuations in the ''conducting'' clusters can also be estimated by Eq. (38).

Because the local fields concentrate in the regions of the closest approach (with the size about a_0) of metal clusters, the averaged fourth power of the local fields can be estimated from Eq. (38) as

$$\langle|E|^4\rangle\propto E_{\rm loc}^4/(l^*)^2=E_0^4(|\varepsilon_m'|/\varepsilon_d)^{2\nu_p/(t+s)}\kappa^{-2\gamma}. \tag{39}$$

Taking into account that in the dielectric gaps with largest local fields $\varepsilon=\varepsilon_d$, we ultimately obtain from Eqs. (22) and (39) the following result for the enhancement of Raman scattering:

$$A\propto(|\varepsilon_m'|/\varepsilon_d)^{2\nu_p/(t+s)}(|\varepsilon_m'|/\varepsilon_m'')^{2\gamma}. \tag{40}$$

Substituting the values of the critical exponents for 2D systems, $t\approx s\approx\nu_p=4/3$ (Refs. 4, 30, and 5) and $\gamma\cong1.0$,[21] we arrive at the following simple formula for the enhanced Raman scattering in a two-dimensional percolation system:

$$A\propto|\varepsilon_m'|^3/(\varepsilon_d\varepsilon_m''^2). \tag{41}$$

If the values of the metal dielectric constant can be approximated by the Drude formula (1), the relation (41), for $\omega_p^*\gg\omega\gg\omega_\tau$, acquires the form

$$A\propto(\omega_p\tau)^2/\varepsilon_d, \tag{42}$$

where $\tau=1/\omega_\tau$ is the relaxation time. According to Eq. (42), at the percolation threshold, the enhancement of Raman scattering in a semicontinuous metal film is independent of the frequency, for the wide spectral range $\omega_p^*\gg\omega\gg\omega_\tau$. This result holds for any semicontinuous film, where the dielectric constant of a conducting component can be approximated by the Drude formula.

There is, of course, a prefactor in Eqs. (41) and (42) that cannot be found from the scaling arguments used above. By comparing results of calculations for Raman scattering following from Eq. (41) and numerical simulations, we find that the prefactor is close to 9.0. Then, Eq. (41) can be rewritten as

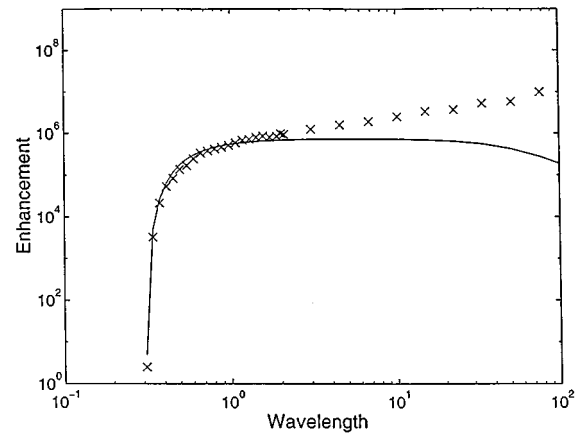

FIG. 5. The enhancement factor A for Raman scattering from a silver semicontinuous film at the percolation threshold. The points are results of the numerical simulations; the solid line represents results of calculations based on Eq. (43).

$$A\approx9.0|\varepsilon_m'|^3/(\varepsilon_d\varepsilon_m''^2). \tag{43}$$

In Fig. 5, we show results of our Monte Carlo simulations for Raman scattering from a silver semicontinuous film at the percolation threshold and results of the calculations based on the formula (43). One can see that Eq. (43) fits the numerical results for almost all the frequencies, such that $\omega\tau\gg1$. At the small frequencies, $\omega\tau\geqslant1$, we observe some deviation from Eq. (43). It is not surprising since the above consideration is based on the assumption that losses are small. We believe that Eq. (43) can be used to estimate the enhancement for Raman scattering from any kind of semicontinuous metal films as well as for other 2D metal-dielectric percolation systems.

To estimate Raman scattering in the case of a three-dimensional percolating system, we should put l^{*3} instead of l^{*2} in Eq. (39). Following then arguments similar to those used to obtain Eq. (41), we find for the enhancement of Raman scattering in 3D the formula

$$A(D=3)\propto\left(\frac{|\varepsilon_m'|}{\varepsilon_d}\right)^{\nu_p/(t+s)}\left(\frac{|\varepsilon_m'|}{\varepsilon''_m}\right)^{2\gamma}. \tag{44}$$

It is difficult to estimate the enhancement of Raman scattering for three-dimensional percolating systems since the critical exponent γ is unknown, in this case. The exponent γ must be positive for a 3D system since the large field fluctuations are anticipated to occur in a 3D network of the L—C elements tuned in resonance with the external field (in the same manner as in 2D systems). On the other hand, the value of the exponent γ for the 3D case probably does not exceed that in the 2D case. This is because in two-dimensional systems the fluctuations are typically larger than in three-dimensional systems. The combination of the critical exponents $\nu_p/(s+t)$ in Eq. (44) is about 1/3 (Refs. 4 and 5) and it is smaller than $2\nu_p/(s+t)\approx1.0$ appearing in Eq. (40) for $D=2$. Therefore the enhancement of Raman scattering given by Eq. (44) can be smaller for a 3D percolating system than in the 2D case. Still, the enhancement of Raman scattering in three-dimensional metal-dielectric systems at the percolation threshold is anticipated to be huge in the visible

and infrared spectral ranges. Observation of Raman scattering in a 3D percolating system could give important information on the field distributions and the nature of the metal-dielectric transition which is still not completely understood (see discussion in Ref. 48, and references therein).

Note that the above results for surface-enhanced Raman scattering from percolation systems are different from those for SERS from fractal aggregates of particles obtained previously by Shalaev and co-workers.[17,18] This is not surprising since a small-particle fractal aggregate is, of course, very different from a percolation system. In particular, for a fractal, $p \to 0$ with the increase of a cluster size, whereas for a homogeneous, on average, percolation system $p \sim 1$. Also, it is worth noting that the fractality provides strong mode localization and therefore the field fluctuations are especially large.[17,47] In accordance with this, SERS from fractals is larger than from percolation systems. We stress that in all the cases, for fractals and percolation systems, the enhancement occurs because of the strong field fluctuations.

Now we evaluate the concentration range where the estimations (40)–(43) for a semicontinuous film are valid. Equations (40)–(43) give the enhancements of Raman scattering at the percolation threshold, $p = p_c$. But they should also be valid in some vicinity of p_c, where the size l^* of the renormalized squares is smaller than the percolation correlation length, $\xi_p \cong a_0(|p-p_c|/p_c)^{-\nu_p}$, that diverges at the percolation threshold. Equating the values of l^* and ξ_p, we obtain the following estimation for the concentration range where the giant enhancement of Raman scattering predicted by Eq. (43) can be observed:

$$|p-p_c|/p_c \leqslant (\varepsilon_d/|\varepsilon_m'|)^{1/(t+s)}. \tag{45}$$

(It is interesting to note that the same range has been estimated in Ref. 31 for the anomalous absorption.) For 2D semicontinuous metal films, the critical exponents are $s \approx t \approx \nu_p = 4/3$, and the above relation acquires the form

$$|p-p_c|/p_c \leqslant (\varepsilon_d/|\varepsilon_m'|)^{3/8}. \tag{46}$$

For the Drude metal, in the frequency range $\omega_p^* \gg \omega \gg \omega_\tau$, relation (46) can be rewritten as

$$|p-p_c|/p_c \leqslant \varepsilon_d^{3/8}(\omega/\omega_p)^{3/4}. \tag{47}$$

As follows from Eq. (47), the concentration range for the enhanced Raman scattering shrinks when the frequency decreases much below the renormalized plasma frequency, $\omega_p^* = \omega_p/\sqrt{\varepsilon_b}$. This result is in agreement with our computer simulations (see Fig. 4).

From the above analysis, it also follows that the results presented in Fig. 5 are valid in a relatively large interval about p_c. It is also interesting to note that the theoretical prediction that SERS is almost frequency independent in the long-wavelength part of the spectrum [see Eq. (42) and Fig. 5] is in agreement with experimental observations.[16,33]

The above scaling analysis for Raman scattering in a percolation system was performed in the quasistatic limit; specifically, we assumed that the skin effect is negligible in the metal grains. As mentioned in the Introduction, in the other limiting case, when the skin effect is very strong and the skin depth δ is much smaller than the grain size, $\delta \ll a_0$, one can represent a metal-dielectric percolating composite as a system of the L — C elements. In this case, the inductance of a metal grain depends on its size and shape, rather than on the values of the metal dielectric constants. The losses in the metal grains are proportional to the ratio $\delta/a_0 \ll 1$, i.e., they are negligible in this case too. Therefore, near the percolation threshold, giant Raman scattering can be observed for any kind of percolating composites, even for the case of strong skin effect. The prime candidates here are composites containing strongly elongated metal inclusions. As shown in Ref. 49, the giant field fluctuations occur in these composites, at least in the microwave range.

As follows from the above discussion, the field intensities in a semicontinuous film, $|E(x,y)|^2$, can be viewed as peaks with the amplitudes $E_{\rm loc}^2$ separated by the distances l^* given by Eqs. (38) and (35), respectively. The amplitudes of the peaks, as well as a typical distance between them, l^*, increase with decreasing frequency, ω. This picture is in qualitative agreement with Figs. 2 and 3.

Note that despite the large distances between the field peaks, $l^* \gg a_0$, the field fluctuations are highly correlated in space. Indeed, the field fluctuations are correlated even for the ''resonance'' system, with the $\varepsilon_m/\varepsilon_d \approx -1 + i\kappa$, as shown in Refs. 20 and 21. The corresponding correlation length is equal to $\xi_e^* \simeq a_0 \kappa^{-\nu_e}$, where $\nu_e \simeq 0.4$ is a critical exponent introduced in Refs. 20 and 21. The correlation length ξ_e tends to infinity, when the system's losses vanish. This correlation length corresponds to the renormalized system. In the original system, the correlation length for the field fluctuations, ξ_e, can be estimated as $\xi_e = \xi_e^*(l^*/a_0) \simeq a_0(\omega_p/\omega)(\omega/\omega_\tau)^{\nu_e}$. Therefore it is much larger than a typical distance between the peaks in the local field distribution. Note that the strong field fluctuations in a semicontinuous film are associated with excitation of the collective eigenmodes of the film.

Raman scattering from a silver semicontinuous film was studied in recent experiments by Gadenne, Gagnot, and Masson[39] (at the wavelength $\lambda = 0.458$ μm). The authors obtained giant enhancements for Raman scattering in the concentration range $\Delta p = 0.55$ around the percolation threshold: $p_c - 0.35 < p < p_c + 0.2$. We use Eq. (46) to estimate the range Δp. Substituting the known values for the dielectric constants of silver grains, $\varepsilon_m = -7.058 + 0.213i$ at $\lambda = 0.470$ μm (Ref. 50) and for a glass substrate, $\varepsilon_d = 2.2$, we obtain $\Delta p \simeq 0.6$, in good agreement with the experimental observations. The experimental results also agree with our calculations shown in Fig. 4. One can see that for the wavelength $\lambda = 0.5$ μm, the SERS has a plateau near p_c. Moreover, our calculations reproduce a fine structure in the enhancement of Raman scattering observed in the experiments. The enhancement has two small maxima, below and above p_c, with a minimum in between. Outside the plateau, Raman scattering drops down by several orders of magnitude. Note that for quantitative comparison with the experiment it is

necessary to multiply the enhancement by the film transmittance squared, $|T_{s,p}(\theta)|^2$ [see Eqs. (28) and (31)]. This will decrease the enhancement for the large metal concentrations, $p \geqslant 0.8$.

As mentioned, the concentration range for the enhancement of Raman scattering is close to the metal concentrations for which the anomalous absorptance is observed.[6,8–10] In Refs. 25, 26, 31, and 51, the anomalous absorptance in a semicontinuous metal film was interpreted as a result of light localization in the film. The em excitations are associated with the resonance collective modes located in different parts of a film. The mode localization also leads to strong field fluctuations over the film.[25,35] Similar arguments were used in Refs. 17, 18, and 31 to explain the enhanced absorption in 3D small-particle composites.

In some cases, one can also observe small peaks in Raman scattering for concentrations far below p_c. We attribute them to the excitation of finite metal clusters. This probably accounts for the experimental results on SERS from the low-concentration granular Ag films.[52]

V. CONCLUSIONS

In this paper we developed a theory expressing Raman scattering in terms of the field fluctuations in inhomogeneous media, such as 2D semicontinuous films. We showed that the enhanced Raman scattering is proportional to the averaged fourth power of the local fields. It follows from the theory that the main sources for the Raman signal are the currents inside the metal grains excited by the Raman-active molecules.

We also studied the field distributions in the near zone of a semicontinuous metal film, for the visible and IR ranges. A very efficient numerical method based on the renormalization group approach is used for direct calculations of the field fluctuations in a percolation system. The local field distributions were then used to calculate the enhanced Raman scattering based on the obtained theoretical formula. We showed that near the percolation threshold of a semicontinuous metal film, Raman scattering is enhanced, on average, by more than six orders of magnitude. The local enhancement can exceed the average one by many orders of magnitude. The enhancement covers a large spectral range, from the visible to the far infrared.

We also performed the scaling analysis for the field fluctuations and obtained analytical expressions for estimating SERS from a semicontinuous metal film. At the percolation threshold, in a wide spectral range, the enhancement is proportional to the square of the product of the plasma frequency and the relaxation time and is independent of the frequency of the applied field. Our scaling analysis shows that the enhancement of Raman scattering is associated with excitations of the collective eigenmodes (consisting of spatially separated sharp peaks) on a semicontinuous film. We also estimated the concentration range near the percolation threshold, where Raman scattering is significantly enhanced. This range shrinks with decreasing the frequency and collapses to the percolation threshold itself in the far-infrared range.

ACKNOWLEDGMENTS

We would like to acknowledge the assistance in computing by O. Lothaire. This research was supported in part by the NSF under Grant No. DMR-9500258 and by NATO under Grants No. CRG-950097 and HTECH.LG951527.

APPENDIX

In this appendix we derive Eq. (7) for the nonlocal conductivity matrix $S^{\alpha\beta}(\mathbf{r}_2,\mathbf{r}_1)$. For this purpose, we rewrite Eq. (4) in the following way:

$$\nabla\cdot[\sigma(\mathbf{r})\nabla\phi(\mathbf{r})]=\nabla\cdot[\sigma(\mathbf{r})\mathbf{E}_e(\mathbf{r})]. \tag{A1}$$

The solution of this equation can be expressed in terms of the Green function G, given by Eq. (6), as

$$\phi(\mathbf{r}_2)=\int G(\mathbf{r}_2,\mathbf{r})\nabla\cdot[\sigma(\mathbf{r})\mathbf{E}_e(\mathbf{r})]d\mathbf{r}. \tag{A2}$$

Integrating in Eq. (A2) by parts, we obtain

$$\phi(\mathbf{r}_2)=-\int \frac{G(\mathbf{r}_2,\mathbf{r})}{\partial r^\beta}[\sigma(\mathbf{r})E_e^\beta(\mathbf{r})]d\mathbf{r}, \tag{A3}$$

where the summation over repeating Greek indices is implied. Substituting the external field $\mathbf{E}_1\delta(\mathbf{r}-\mathbf{r}_1)$ applied at the coordinate $\mathbf{r}_1$ and integrating over the coordinate $\mathbf{r}$, we obtain

$$\phi(\mathbf{r}_2)=-\sigma(\mathbf{r}_1)\frac{G(\mathbf{r}_2,\mathbf{r}_1)}{\partial r_1^\beta}E_1^\beta \tag{A4}$$

for the potential at the coordinate $\mathbf{r}_2$. The current density at the coordinate $\mathbf{r}_2$ is equal to

$$j^\alpha(\mathbf{r}_2)=\sigma(\mathbf{r}_2)\sigma(\mathbf{r}_1)\frac{G(\mathbf{r}_2,\mathbf{r}_1)}{\partial r_2^\alpha\partial r_1^\beta}E_1^\beta. \tag{A5}$$

Comparing this equation with the definition of the nonlocal conductivity $\hat{S}$ given by Eq. (5), we arrive at Eq. (7), which expresses the nonlocal conductivity in terms of the Green function G.

Below, we show how Eq. (20) can be obtained from Eq. (19). For this, we rewrite Eq. (20) in the form

$$\langle I_s\rangle\propto\frac{|\kappa|^2}{|E_0|^2}\int|\sigma(\mathbf{r})|^2E^\alpha(\mathbf{r})E^{*\alpha}(\mathbf{r})E^\beta(\mathbf{r})E^{*\beta}(\mathbf{r})d\mathbf{r}, \tag{A6}$$

where the integration is over the entire film plane. Using Eq. (9), we can rewrite Eq. (A6) in terms of the applied field E_0^α as

$$\langle I_s\rangle\propto\frac{|\kappa|^2}{|E_0|^2}\int|\sigma(\mathbf{r})|^{-2}S^{\alpha\gamma}(\mathbf{r},\mathbf{r}_1)S^{*\alpha\delta}(\mathbf{r},\mathbf{r}_2)\times S^{\beta\lambda}(\mathbf{r},\mathbf{r}_3)S^{*\beta\mu}(\mathbf{r},\mathbf{r}_4)E_0^\gamma E^{*\delta}_0E_0^\lambda E^{*\mu}_0d\mathbf{r}_1d\mathbf{r}_2d\mathbf{r}_3d\mathbf{r}_4d\mathbf{r}. \tag{A7}$$

For the macroscopically isotropic systems considered here, Raman scattering does not depend on the direction of the applied field $\mathbf{E}_0$. Therefore we can average Eq. (A7) over the orientations of the field $\mathbf{E}_0$, without changing the result. The only term in Eq. (A7) to be averaged over the orientations is the product $E_0^{\gamma}E^{*\delta}_0E_0^{\lambda}E^{*\mu}_0$ since the nonlocal conductivity matrix $\hat{S}$ defined by Eq. (5) is independent of the field $\mathbf{E}_0$. The applied field $\mathbf{E}_0$ is supposed to be linearly polarized and therefore its amplitude can be chosen to be real. Thus we obtain $E_0^{\gamma}E^{*\delta}_0E_0^{\lambda}E^{*\mu}_0=E_0^{\gamma}E_0^{\delta}E_0^{\lambda}E_0^{\mu}$. After the averaging over the orientations this product takes the form

$$\langle E_0^{\gamma}E_0^{\delta}E_0^{\lambda}E_0^{\mu}\rangle_0=\frac{1}{2}(\langle E_0^{\gamma}E_0^{\delta}\rangle_0\langle E_0^{\lambda}E_0^{\mu}\rangle_0+\langle E_0^{\gamma}E_0^{\lambda}\rangle_0\langle E_0^{\delta}E_0^{\mu}\rangle_0 +\langle E_0^{\gamma}E_0^{\mu}\rangle_0\langle E_0^{\delta}E_0^{\lambda}\rangle_0). \tag{A8}$$

Substituting the decomposed average $\langle E_0^{\gamma}E^{*\delta}_0E_0^{\lambda}E^{*\mu}_0\rangle_0$ in Eq. (A7) and integrating over the coordinates $\mathbf{r}_1,\mathbf{r}_2,\mathbf{r}_3,\mathbf{r}_4$, we obtain Eq. (19). This proves that Eqs. (19) and (20) are equivalent.

[1] R.W. Cohen, G.D. Cody, M.D. Coutts, and B. Abeles, Phys. Rev. B **8**, 3689 (1973).

[2] G.A. Niklasson and C.G. Granqvist, J. Appl. Phys. **55**, 3382 (1984).

[3] J.P. Clerc, G. Giraud, and J.M. Luck, Adv. Phys. **39**, 191 (1990).

[4] D. Stauffer and A. Aharony, *Introduction to Percolation Theory*, 2nd ed. (Taylor and Francis, Philadelphia, 1991).

[5] D.J. Bergman and D. Stroud, in *Solid State Physics: Advances in Research and Applications* (Academic, New York, 1992), Vol. 46, p. 147.

[6] Y. Yagil, P. Gadenne, C. Julien, and G. Deutscher, Phys. Rev. B **46**, 2503 (1992).

[7] T.W. Noh, P.H. Song, Sung-Il Lee, D.C. Harris, J.R. Gaines, and J.C. Garland, Phys. Rev. B **46**, 4212 (1992).

[8] P. Gadenne, A. Beghadi, and J. Lafait, Opt. Commun. **65**, 17 (1988).

[9] P. Gadenne, Y. Yagil, and G. Deutscher, J. Appl. Phys. **66**, 3019 (1989).

[10] Y. Yagil, M. Yosefin, D.J. Bergman, G. Deutscher, and P. Gadenne, Phys. Rev. B **43**, 11 342 (1991).

[11] J.C. Maxwell-Garnett, Philos. Trans. R. Soc. London **203**, 385 (1904).

[12] D.A.G. Bruggeman, Ann. Phys. (Leipzig) **24**, 636 (1935).

[13] F. Brouers, J.P. Clerc, and G. Giraud, Phys. Rev. B **44**, 5299 (1991); F. Brouers, J.M. Jolet, G. Giraud, J.M. Laugier, and Z.A. Randriamanantany, Physica A **207**, 100 (1994).

[14] A.P. Vinogradov, A.M. Karimov, and A.K. Sarychev, Zh. Eksp. Teor. Fiz. **94**, 301 (1988) [Sov. Phys. JETP **67**, 2129 (1988)].

[15] G. Depardieu, P. Frioni, and S. Berthier, Physica A **207**, 110 (1994).

[16] M. Moskovits, Rev. Mod. Phys. **57**, 783 (1985).

[17] V.M. Shalaev, Phys. Rep. **272**, 61 (1996).

[18] V.M. Shalaev, E.Y. Poliakov, and V.A. Markel, Phys. Rev. B **53**, 2437 (1996); V.A. Markel, V.M. Shalaev, E.B. Stechel, W. Kim, and R.L. Armstrong, *ibid.* **53**, 2425 (1996); M.I. Stockman, V.M. Shalaev, M. Moskovits, R. Botet, and T.F. George, *ibid.* **46**, 2821 (1992).

[19] L.D. Landau and E.M. Lifshitz, *Electrodynamics of Continuous Media*, 2nd ed. (Pergamon Press, Oxford, 1984).

[20] F. Brouers, S. Blacher, and A. K. Sarychev, in *Fractals in the Natural and Applied Sciences*, edited by M.M. Novak (Chapman and Hall, London, 1995), Chap. 24.

[21] F. Brouers, S. Blacher, and A. K. Sarychev (unpublished).

[22] D.J. Bergman, O. Levy, and D. Stroud, Phys. Rev. B **49**, 129 (1994).

[23] D.P. Tsai *et al.*, Phys. Rev. Lett. **72**, 4149 (1994).

[24] S.I. Bozhevolnyi, I.I. Smolyaninov, and A.V. Zayats, Phys. Rev. B **51**, 17 916 (1995).

[25] A.K. Sarychev, D.J. Bergman, and Y. Yagil, Physica A **207**, 372 (1994).

[26] A.K. Sarychev, D.J. Bergman, and Y. Yagil, Phys. Rev. B **51**, 5366 (1995).

[27] A.N. Lagarkov, N.K. Rosanov, A. K. Sarychev, and K. Simonov, in Proceedings of the International Conference: ETOPIM4, St. Petersburg-Moscow, July 23–30, 1996 [Physica A (to be published)].

[28] D.J. Bergman and R. Levy-Nathansohn, in Proceedings of the International Conference: ETOPIM4, St. Petersburg-Moscow, July 23–30, 1996 [Physica A (to be published)].

[29] X. C. Zeng, P.M. Hui, and D. Stroud, Phys. Rev. B **39**, 1063 (1989).

[30] J. P. Clerc, G. Giraud, and J. M. Luck, Adv. Phys. **39**, 191 (1990).

[31] F. Brouers, J.P. Clerc, and G. Giraud, Phys. Rev. B **47**, 666 (1993).

[32] A.M. Dykhne, Zh. Eksp. Teor. Fiz. **59**, 110 (1970) [Sov. Phys. JETP **32**, 348 (1971)].

[33] *Surface Enhanced Raman Scattering*, edited by R.K. Chang and T.E. Furtak (Plenum Press, New York, 1982).

[34] V.M. Shalaev, R. Botet, J. Mercer, and E.B. Stechel, Phys. Rev. B **54**, 8235 (1996).

[35] E.Y. Poliakov, V.M. Shalaev, and V.A. Markel, Opt. Lett. **21**, 1628 (1996).

[36] R. Chiarello, V. Panella, J. Krim, and C. Thompson, Phys. Rev. Lett. **67**, 3408 (1991).

[37] C. Douketis, Z. Wang, T.L. Haslet, and M. Moskovits, Phys. Rev. B **51**, 11 022 (1995).

[38] A.-L. Barabasi and H.E. Stanley, *Fractal Concepts in Surface Growth* (Cambridge University Press, Cambridge, England, 1995); *Dynamics of Fractal Surfaces*, edited by F. Family and T. Vicsek (World Scientific, Singapore, 1991).

[39] P. Gadenne, D. Gagnot, and M. Masson, in Proceedings of the International Conference: ETOPIM4, St. Petersburg-Moscow, July 23–30, 1996 [Physica A (to be published)].

[40] M.A. Tadayoni and N.R. Dando, Appl. Spectrosc. **45**, 1613 (1991).

[41] P.J. Reynolds, W. Klein, and H.E. Stanley, J. Phys. C **10**, L167 (1977).

[42] A.K. Sarychev, Zh. Eksp. Teor. Fiz. **72**, 1001 (1977) [Sov. Phys. JETP **45**, 524 (1977)].

[43] J. Bernasconi, Phys. Rev. B **18**, 2185 (1978).

[44] A. Aharony, Physica A **205**, 330 (1994).
[45] D. J. Frank and C.J. Lobb, Phys. Rev. B **37**, 302 (1988).
[46] *Handbook of Optical Constants of Solids*, edited by E.D. Palik (Academic Press, New York, 1985).
[47] M.I. Stockman, L.N. Pandey, L.S. Muratov, and T.F. George, Phys. Rev. Lett. **72**, 2486 (1994); V.A. Markel, L.S. Muratov, M.I. Stockman, and T.F. George, Phys. Rev. B **43**, 8183 (1991).
[48] A.K. Sarychev and F. Brouers, Phys. Rev. Lett. **73**, 2895 (1994).
[49] A.N. Lagarkov and A.K. Sarychev, Phys. Rev. **53**, 6318 (1996).
[50] P.B. Johnson and R.W. Christy, Phys. Rev. B **6**, 4370 (1972).
[51] F. Brouers, D. Rauw, J.P. Clerc, and G. Giraud, Phys. Rev. B **49**, 14 582 (1994).
[52] J.G. Bergman, D.S. Chempla, P.F. Liap, A.M. Glass, A. Pinezuk, R.M. Hart, and D.H. Olson, Opt. Lett. **6**, 33 (1981).